ACES Asian Chemical Editorial Society

doi.org/10.1002/asia.202300673

CHEMISTRY AN ASIAN JOURNAL Research Article

www.chemasianj.org

Special Collection

Stoichiometric Control of Guest Recognition of Self-Assembled Palladium(II)-Based Supramolecular Architectures

Jess L. Algar,[a] James E. Phillips,[a] Jack D. Evans,[b] and Dan Preston*[a]

We report flexible $[Pd(\mathbf{L})_2]^{2+}$ complexes where there is self-recognition, driven by π-π interactions between electron-rich aromatic arms and the cationic regions they are tethered to. This self-recognition hampers the association of these molecules with aromatic molecular targets in solution. In one case, this complex can be reversibly converted to an 'open' $[Pd_2(\mathbf{L})_2]^{4+}$ macrocycle through introduction of more metal ion. This is accomplished by the ligand having two bidentate binding sites: a 2-pyridyl-1,2,3-triazole site, and a *bis*-1,2,3-triazole site. Due to favourable hydrogen bonding, the 2-pyridyl-1,2,3-triazole units reliably coordinate in the $[Pd(\mathbf{L})_2]^{2+}$ complex to control speciation: a second equivalent of Pd(II) is required to enforce coordination to *bis*-triazole sites and form the macrocycle. The macrocycle interacts with a molecular substrate with higher affinity. In this fashion we are able to use stoichiometry to reversibly switch between two different species and regulate guest binding.

Introduction

A central component of the power of naturally occurring machines such as peptides and proteins to interact with molecular targets is the capacity of the activity of these molecules to be regulated. This regulation allows these hosts to spring into action when most needed, and is often accomplished through a stimulus bringing about conformational or similar shift that alters the capacity of the host to interact with its target.[1]

Synthetic chemists are attempting to create artificial molecules[2] with similar capabilities for roles such as molecular transformation,[3] molecular delivery/transport,[4] and sequestration.[5] Naturally, the ability for this capability to be likewise regulated would be advantageous, so switchable systems have become an area of keen interest for metallo-supramolecular chemists.[6] Chemists have been able to alter or switch structure using a variety of stimuli, including concentration and temperature,[7] solvent,[8] redox state,[9] acid/base chemistry,[10] ligand competition,[11] allostery-driven interconversions,[12] and light.[13]

Stoichiometry has also been used, where chemical species have been interconverted between two or more states by stepwise addition of one or more components. This includes work from Yoshizawa and co-workers converting between a $[Hg_2(\mathbf{L})_2]^{2+}$ macrocycle and a $[Hg_2(\mathbf{L})_4]^{2+}$ lantern-shaped cage,[14] by Chand and co-workers who have switched between a $[Pd(\mathbf{L})_2]^{2+}$ spiro-type complex and a double cavity $[Pd_3(\mathbf{L})_4]^{6+}$ cage,[15] and recently by Nitschke and co-workers in the conversion from a $[Pd_3(\mathbf{L})(\mathbf{L}')(solvent)_3]^{6+}$ species to a $[Pd_{12}(\mathbf{L})_4(\mathbf{L}')_8]^{24+}$ cage.[16] We have also used stoichiometry to switch between $[Pd_n(\mathbf{L})_2]^{2n+}$ species where $n = 1$, 2 or 4,[17] and combined this with concentration dependence to switch between a mononuclear $[Pd(\mathbf{L})_2]^{2+}$ complex, a $[Pd_2(\mathbf{L})_2]^{4+}$ dimer, and a $[Pd_9(\mathbf{L})_{12}]^{18+}$ cage.[18]

Most of the examples given above relate to systems where the species or states accessed are rigid in character. But switchability has also been incorporated into flexible systems, using acid/base chemistry,[19] the presence or absence of a metal ion,[20] or charge.[21] We are interested in systems that have a degree of flexibility,[22] which often rely upon π-π interactions to enforce their persistent conformation.[23] These π-π interactions are similarly useful for molecular recognition events, and are accentuated between electron-rich aromatic guests and electron deficient hosts, with the cationic regions of the host particularly well suited to carrying out this role.[24]

Here we report a system where the planar cationic panels of palladium(II) complexes have affinity for electron rich aromatic molecular targets. This can be disrupted through covalently tethering aromatic groups to the complexes with flexible diethylene glycol chains. The entropic result of tethering the components together increases the strength of the interactions

[a] J. L. Algar, J. E. Phillips, Dr. D. Preston
Research School of Chemistry
Australian National University
Canberra ACT 2600 (Australia)
E-mail: daniel.preston@anu.edu.au

[b] Dr. J. D. Evans
Centre for Advanced Nanomaterials and Department of Chemistry
The University of Adelaide
Adelaide, SA 5000 (Australia)

Supporting information for this article is available on the WWW under https://doi.org/10.1002/asia.202300673

This manuscript is a contribution to a Joint Early Career Researcher Special Collection published by Chemistry – An Asian Journal, ChemNanoMat and the Asian Journal of Organic Chemistry.

between these components, resulting in effective competition between the tethered aromatic groups and aromatic targets. We have an interest in tailoring metal binding sites on ligands to come together in specific ways,[25] and here have been able to use *bis*-bidentate ligands with differentiated bidentate sites, to form $[Pd(\mathbf{L})_2]^{2+}$ complexes where one bidentate site coordinates and the other does not. Instead, the secondary bidentate sites act as the aromatic region competing with 9-methylanthracene guests, consequently lowering their binding affinity. Introduction of another equivalent of palladium(II) results in coordination to the second bidentate site, and the formation of a 2+2 macrocycle. Given the cationic faces of this species are now 'open', it has a higher affinity for 9-methylanthracene. This process can be reversed by adding more of the ligand.

Results and Discussion

Model System: Testing Self-recognition

In our planned system, aromatic groups tethered to the cationic center of the complex were planned to occlude access to these cationic panels through competition. We therefore firstly checked this hypothesis using a model ligand $\mathbf{L_{nap}}$ (Figure 1, *ligands*). It incorporated at one end a 2-pyridyl-1,2,3-triazole bidentate chelator, which has previously been demonstrated to form *bis*-bidentate complexes with square planar metal ions in a head-to-tail fashion (Figure 1 *pairings left*).[26] This head-to-tail arrangement around the metal ion is driven through complementary hydrogen bonding between the N2 nitrogen of the triazole, and the hydrogen *ortho* to the coordinating nitrogen on the pyridine. At the other end of the ligand was a naphthalene group, which was attached to the bidentate site through a diethylene glycol linker. It was hypothesised that the electron-rich aromatic group would sit over the electron-deficient panel after complexation due to favourable π-π interactions between the two components, accentuated by the tethering together of the two components. It was intended that the self-recognition would impair guest binding.

The combination of one equivalent of $[Pd(CH_3CN)_4](BF_4)_2$ with two equivalents of $\mathbf{L_{nap}}$ gave a single set of peaks in the ^{1}H Nuclear Magnetic Resonance (NMR) spectrum (Figure 2c) suggesting only a single species was present, as was confirmed by ^{1}H Diffusion Ordered Spectroscopy (DOSY) NMR where all peaks were diffusing with a single coefficient ($D = 8.62\times10^{-10}$ m^2 s^{-1}). In comparison to the spectrum of the 'free' ligand, downfield shifting of the resonances of ligand proton environments surrounding the metal binding site was observed. For example, proton H_a shifted downfield by 0.16 ppm (Supporting Information, Figure S1.11). This was indicative of metal coordination, suggesting $[Pd(\mathbf{L_{nap}})_2](BF_4)_2$ had successfully been produced (Supporting Information, Figure 2.1). The complex was additionally identified via High Resolution Electrospray ionisation-Mass Spectrometry (HR ESI-MS), m/z = 413.1112 $[M]^{2+}$ (calc. for $C_{42}H_{40}N_8O_4Pd$, 413.1111) and m/z = 913.2245 $[MBF_4]^+$ (calc. for $C_{42}H_{39}BF_4N_8O_4Pd$, 913.2257) (Supporting Information, S1.2.3.1).

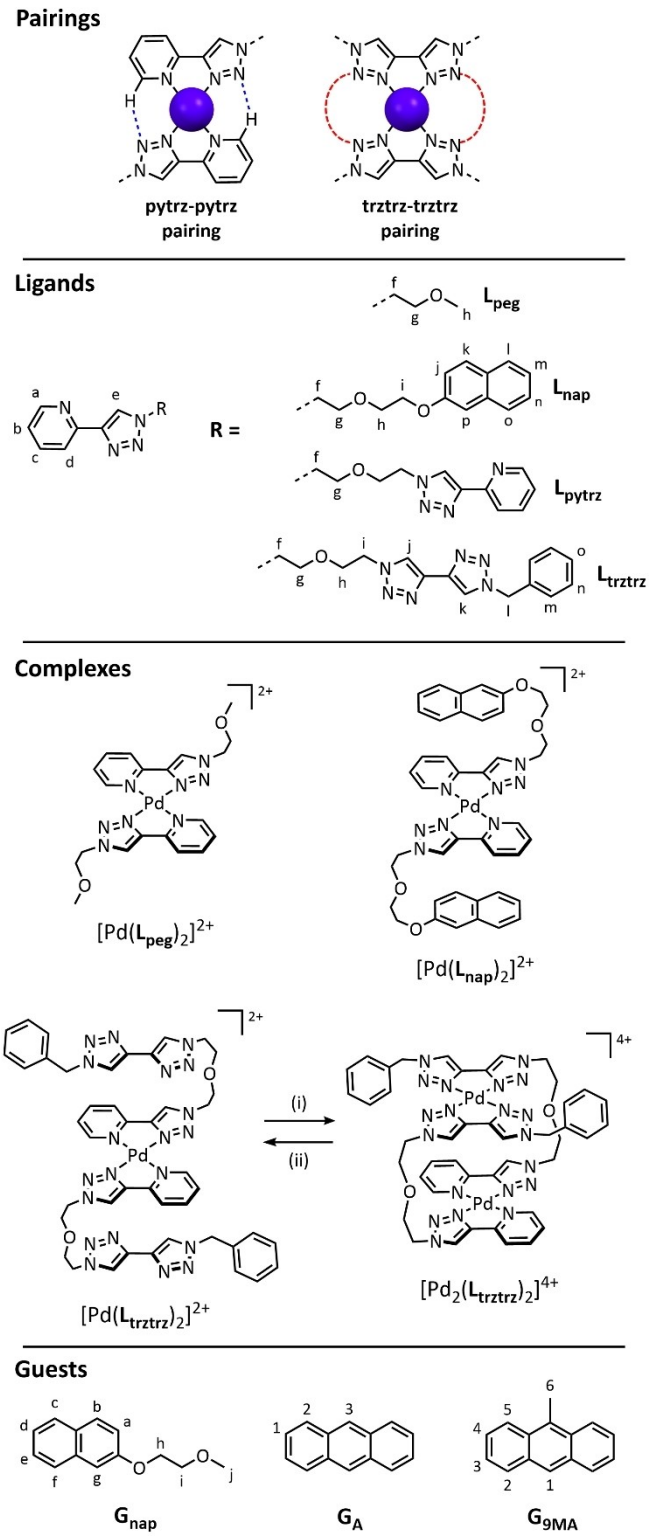

Figure 1. Chemical structures of pairings, ligands, complexes and guests used in this study. In the depiction of the pairings, favourable hydrogen-bonding interactions are shown with blue dotted lines, and unfavourable lone pair-lone pair interactions with red dotted lines.

Upfield shifting of ^{1}H NMR spectral environments is indicative of π-π interactions, and we hoped to use this to gauge the extent to which the naphthalene was associating

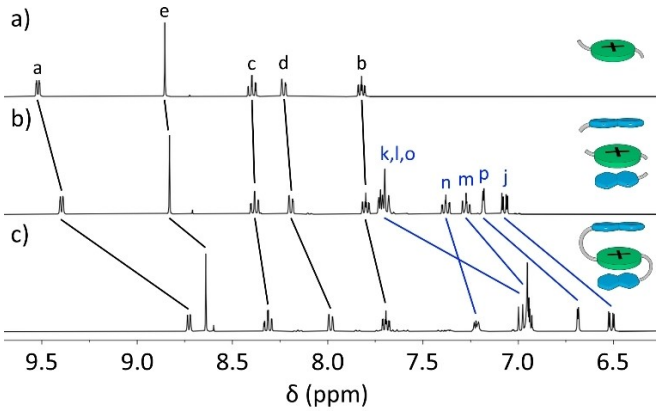

Figure 2. Partial ^{1}H NMR spectra (400 MHz, CD_3CN, 298 K) depicting chemical shifts between environments of a) the complex $[Pd(\mathbf{L_{peg}})_2]^{2+}$, b) $[Pd(\mathbf{L_{peg}})_2]^{2+}$ with 2 equivalents of $\mathbf{G_{nap}}$ and c) the complex $[Pd(\mathbf{L_{nap}})_2]^{2+}$. Labelling is taken from ligand $\mathbf{L_{nap}}$, labels in black corresponding to environments from the 2-pyridyl-1,2,3-triazole region, labels in blue to the naphthalene region.

with the cationic panel. However, to do this we had to differentiate between intra- and inter-molecular association.

Accordingly, we also synthesised ligand $\mathbf{L_{peg}}$, which consisted of the 2-pyridyl-1,2,3-triazole chelator with a simple monomethyl(ethylene) glycol substituent, and an 'untethered' naphthalene ($\mathbf{G_{nap}}$) which also had a short monomethyl(ethylene) glycol substituent. Combining these gives a system which could represent ligand $\mathbf{L_{nap}}$ with the glycol chain severed, i.e. with the entropic benefits of high effective concentration removed. The ligand $\mathbf{L_{peg}}$, its complex $[Pd(\mathbf{L_{peg}})_2](BF_4)_2$ and $\mathbf{G_{nap}}$ were all synthesized and analysed by standard techniques (Supporting Information S1.2.2.2, S1.2.3.2, S4.1), including, for the complex, X-ray crystallography, which showed the intended head-to-tail organization of ligands around the Pd(II) metal center (Figure 3a).[27]

We were now able use ^{1}H NMR spectroscopy to make a direct comparison between the simple complex $[Pd(\mathbf{L_{peg}})_2]^{2+}$ both by itself and with 2 equivalents of $\mathbf{G_{nap}}$, and $[Pd(\mathbf{L_{nap}})_2]^{2+}$. The addition of 2 equivalents of $\mathbf{G_{nap}}$ to a 7.5 mM solution of

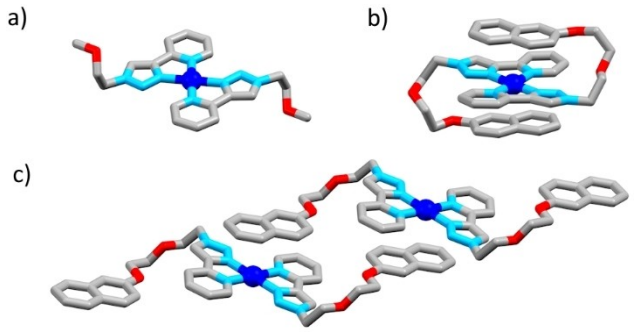

Figure 3. Depictions of structures of a) $[Pd(\mathbf{L_{peg}})_2]^{2+}$ (X-ray structure), b) $[Pd(\mathbf{L_{nap}})_2]^{2+}$ (DFT simulations) with a conformation consistent with solution phase data, and c) two of the $[Pd(\mathbf{L_{nap}})_2]^{2+}$ complexes in the crystal depicting π-π interactions between naphthalene arms and cationic panels of the adjacent complex. Colours: carbon grey, nitrogen blue, oxygen red, palladium dark blue. Hydrogen atoms and counterions omitted for clarity.

the $[Pd(\mathbf{L_{peg}})_2]^{2+}$ complex resulted in slight upfield shifting of the peaks of the cationic panel environments, specifically by 0.12 ppm for H_a (Figure 2a and b). Therefore, while π-π interactions exist between $\mathbf{G_{nap}}$ and the complex, they are weak in nature. Quantitative measurements from binding titrations revealed the binding constant between $[Pd(\mathbf{L_{peg}})_2]^{2+}$ and $\mathbf{G_{nap}}$ was extremely low ($K_{11} = 8.0 \pm 0.3\ M^{-1}$).[28] In comparison, the upfield shifting was much more significant in the intramolecular model complex, $[Pd(\mathbf{L_{nap}})_2]^{2+}$ (Figure 2c). For example, the resonance of proton H_a has shifted further upfield by 0.67 ppm and the resonances of protons H_k, H_l and H_o (overlapping environments) have shifted upfield by approximately 0.75 ppm relative to the solution of $[Pd(\mathbf{L_{peg}})_2]^{2+}$ and $\mathbf{G_{nap}}$. Therefore, the π-π interactions between the cationic panel and tethered naphthalene are more persistent than that mimicked by the intermolecular system. This behaviour can be accounted for by entropic reasons; if the cationic panel and aromatic group are tethered together, their opportunity for π-π interactions will increase due to their increased effective concentration. Confirmation that the π-π interactions observed in the ^{1}H NMR spectra were indeed intramolecular (i.e. self-recognition) was obtained by diluting a 7.5 mM ^{1}H NMR sample of $[Pd(\mathbf{L_{nap}})_2]^{2+}$ by a factor of 10 (Supporting Information Figure 1.12). This induced no change in the chemical shift of any proton environments. Furthermore, a ^{1}H NOESY NMR spectrum identified through-space NOE correlations between proton environments on the cationic panel and proton environments on the aromatic tether. Specifically, couplings were observed between protons H_e and H_j, H_e and H_k, H_l, H_m, H_o, (overlapping environments), H_e and H_n, H_a and H_p, H_a and H_n, H_d and H_j and finally between H_d and H_k, H_l, H_m, H_o (see Supporting Information Figure 1.13).

Colourless, block-like single crystals were obtained for both $[Pd(\mathbf{L_{nap}})_2](BF_4)_2$ (space groups $P2_1/n$) via vapour diffusion of diethyl ether into an acetonitrile solution of the complex. The solution of the X-ray diffraction data which was collected confirmed the identity of the intended complex, with the expected head-to-tail conformation about palladium(II) in order to maximise hydrogen bonding (Figure 3c). At the 'infinite' concentration in the lattice, there were π-π interactions evident between the cationic panel and the naphthalene groups of neighbouring molecules, demonstrating the capacity for these components to interact. To obtain a representative structure of the complex in solution, computational methods (DFT simulations, BP86 functional, def2-TZVPP for Pd and N, def2-SVP for all other atoms) were used. An optimised structure (Figure 3b) revealed the expected self-recognition between the cationic panel and aromatic tethers and is in accordance with the observed through-space NOE couplings.

Model System: Impairing Guest Recognition

Having shown that tethering naphthalene groups to the 2-pyridyl-1,2,3-triazole group of $\mathbf{L_{nap}}$ led to enhanced recognition between these components in the resulting complex, we now sought to establish that this self-recognition would impede

molecular recognition between the cationic panel of the complex and other molecular guests in solution. Two guests were investigated: 9-methylanthracene ($\mathbf{G_{9MA}}$) and anthracene ($\mathbf{G_A}$). Again, we used the naphthalene substituted system $[Pd(\mathbf{L_{nap}})_2]^{2+}$ with comparison to the model complex $[Pd(\mathbf{L_{peg}})_2]^{2+}$ to discern the impact of the tethered aromatic groups, and in turn assess the effect of self-recognition.

The addition of two equivalents of $\mathbf{G_{9MA}}$ to the complex $[Pd(\mathbf{L_{peg}})_2]^{2+}$ resulted in upfield shifting of the peaks corresponding to $\mathbf{G_{9MA}}$, indicative of π-π interactions between the cationic panel of the model complex and the guest. The same addition to the self-recognising complex $[Pd(\mathbf{L_{nap}})_2]^{2+}$ resulted in only minor upfield shifting by comparison. The average magnitude of upfield shifting decreased from 0.16 ppm to only 0.03 ppm (over a five-fold decrease) between $[Pd(\mathbf{L_{peg}})_2]^{2+}$ and $[Pd(\mathbf{L_{nap}})_2]^{2+}$ respectively (Supporting Information, Figure 2.5). ^{1}H NMR binding titrations supported the initial ^{1}H NMR analysis as K_{11} decreased nearly four-fold (from $162 \pm 3\ M^{-1}$ to $44.1 \pm 0.5\ M^{-1}$) between $\mathbf{G_{9MA}}$ and the two complexes (1:2 statistical binding mode, Supporting Information S3.1 and S3.2). Similar results in terms of the magnitude of chemical shifts were observed with $\mathbf{G_A}$, but its poor solubility precluded ^{1}H NMR titrations. Unfortunately, host guest adducts were not observed for any of the systems in this study *via* mass spectrometry, unsurprisingly considering the magnitude of the binding constants.

Stoichiometry Dependent System

Having confirmed that tethering aromatic groups to the complex impaired guest recognition, we next investigated whether we could use stoichiometry-responsive groups instead of naphthalene. We therefore synthesised a new ligand, $\mathbf{L_{tztz}}$ (Figure 1). As with previous ligands in this series, this ligand had a 2-pyridyl-1,2,3-triazole chelator at one end. However, tethered to this group through a diethylene glycol chain, was an additional coordination site. This secondary coordination site was a *bis*-triazole. Unlike a 2-pyridyl-1,2,3-triazole, which can be incorporated into a *bis*-bidentate complex with two favourable hydrogen bonds, *bis*-bidentate *bis*-triazole complexes have the lone pairs from their N2 nitrogen atoms directed towards each other (Figure 1 *pairings right*). Through the use of this low symmetry *bis*-bidentate ligand, we hoped therefore to be able to control the assembly process between two ligands and one metal ion so that only the 2-pyridyl-1,2,3-triazoles were coordinated to the metal ion, and the uncomplexed *bis*-triazoles would associate and in turn occlude the cationic panel through π-π interactions. The combination of one equivalent of $[Pd(CH_3CN)_4](BF_4)_2$ with two equivalents of $\mathbf{L_{trztrz}}$ produced a single set of resonances per ligand environment in the ^{1}H NMR spectrum; all peaks were diffusing at the same rate as established through ^{1}H DOSY spectroscopy ($D = 5.88\times10^{-10}\ m^2\ s^{-1}$). Downfield shifting of peaks pertaining to pyridyl-triazole environments and upfield or minor shifting of *bis*-triazole environments relative to free $\mathbf{L_{trztrz}}$ indicated that coordination existed exclusively about the pyridyl-triazole sites to give the self-recognising species, $[Pd(\mathbf{L_{trztrz}})_2]^{2+}$ (Supporting Information, Figure 2.3). This was additionally identified via HR ESI-MS (CD_3CN/CH_3CN), $m/z = 495.1534$ $[M]^{2+}$ (calc. for $C_{44}H_{44}N_{20}O_2Pd$, 495.1503) and $m/z = 1077.3036$ $[MBF_4]^+$ (calc. for $C_{44}H_{44}{}^{11}BF_4N_{20}O_2Pd$, 1077.3041). Upfield shifting of the peaks from the cationic panel environments of $[Pd(\mathbf{L_{trztrz}})_2]^{2+}$ relative to $[Pd(\mathbf{L_{peg}})_2]^{2+}$ indicated that self-recognition existed in the former (Figure 4a and b).

For comparison, we carried out the same experiment using another analogous *bis*-bidentate ligand ($\mathbf{L_{pytrz}}$, Figure 1) which had two 2-pyridyl-1,2,3-triazole chelators linked by the diethylene glycol chain. The 2:1 combination of this ligand with palladium(II) in CD_3CN resulted in an untidy spectrum (Supporting Information Figure S2.5) containing three species: the free ligand, the $[Pd(\mathbf{L_{pytrz}})_2]^{2+}$ complex, and a dinuclear $[Pd_2(\mathbf{L_{pytrz}})_2]^{2+}$ dimer (see below). These three species were also evident in the mass spectrum obtained for the mixture (Supporting Information Figure 2.6). We were therefore able to directly attribute the formation of a single species with ligand $\mathbf{L_{trztrz}}$ to the differentiation between its two bidentate sites.

We next added a second equivalent of palladium(II) to $[Pd(\mathbf{L_{trztrz}})_2]^{2+}$. After addition, the mononuclear species was no long observed, and there was conversion to a different set of peaks in the ^{1}H NMR spectrum (Figure 4c). There was a small amount of untidiness in the spectrum, but >95% by integration was a single set of peaks per ligand environment. In this set, the peaks from the *bis*-triazole unit had shifted downfield, consistent with complexation. This new species had a larger diffusion coefficient of ($D = 6.85\times10^{-10}\ m^2/s$) than $[Pd(\mathbf{L_{trztrz}})_2]^{2+}$, consistent with this new species having a smaller solvodynamic radius. HR ESI-MS on the system revealed a species of $[Pd_2(\mathbf{L_{trztrz}})_2]^{4+}$ composition, e.g. $m/z = 395.0697$ $[MBF_4]^{3+}$ (calc. for $C_{44}H_{44}BF_4N_{20}O_2Pd_2$, 395.0695), $m/z = 636.1063$ $[M(BF_4)_2]^{2+}$ (calc. for $C_{44}H_{44}B_2F_8N_{20}O_2Pd_2$, 636.1061) and $m/z = 1358.2170$ $[M(BF_4)_3]^{1+}$ (calc. for $C_{44}H_{44}B_3F_{12}N_{20}O_2Pd_2$, 1358.2162).

The presence of >95% by integration being a single set of peaks per ligand environment in the spectrum for $[Pd_2(\mathbf{L_{trztrz}})_2]^{4+}$ indicated the predominant formation of a single isomer. Leaving the sample at either room temperature or at 80 °C for

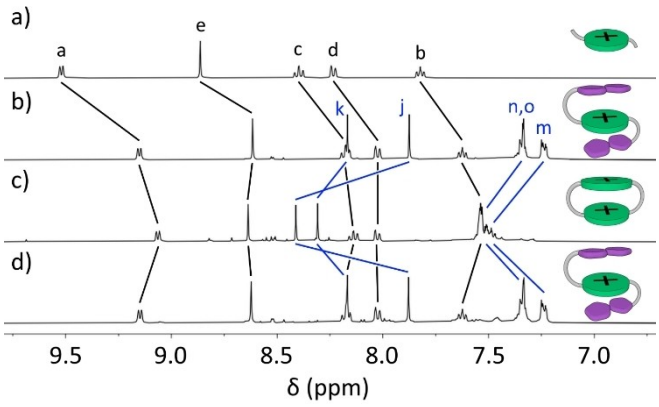

Figure 4. Partial ^{1}H NMR spectra (400 MHz, CD_3CN, 298 K) of a) $[Pd(\mathbf{L_{peg}})_2]^{2+}$, b) $[Pd(\mathbf{L_{trztrz}})_2]^{2+}$, c) $[Pd(\mathbf{L_{trztrz}})_2]^{2+}$ + 1 equivalent of Pd(II) giving $[Pd_2(\mathbf{L_{trztrz}})_2]^{4+}$ and d) $[Pd_2(\mathbf{L_{trztrz}})_2]^{4+}$ + 2 equivalents of $\mathbf{L_{trztrz}}$ giving $[Pd(\mathbf{L_{trztrz}})_2]^{2+}$.

long periods of time led to no alteration to the spectral intensities suggesting that this was the thermodynamic product. The presence of an *AB* quartet for the methylene environment H_l (Supporting Information Figure S1.26) suggested that the macrocycle was formed with the two cationic panels face to face, causing desymmetrisation. Likewise, the upfield shifts of the complex in comparison to $[Pd(\mathbf{L_{peg}})_2]^{2+}$ suggested a face-to-face isomer resulting in π-π interactions. Surveying four possible isomers (*syn/anti* combinations with the binding sites either matched or mixed) of $[Pd_2(\mathbf{L_{trztrz}})_2]^{4+}$ using DFT we found the *anti* and *syn* conformations can fall within a free energy difference of 10 kJ/mol. The conformational landscape of these dimers is complex (far greater than the four conformers considered here) and we are currently developing advanced methodologies to explore the structural diversity of Pd(II) macrocycle complexes. We were able to grow crystals of the complex from vapour diffusion of diethyl ether into an acetonitrile solution of it. The solution from the data obtained from these revealed the macrocyclic structure of $[Pd_2(\mathbf{L_{trztrz}})_2]^{4+}$ to indeed be face-to-face, consistent with the NMR data (Figure 5a). The bidentate sites of each ligand were orientated in a *syn* position to each other, and the two palladium(II) ions were 3.346(2) Å from one another. One metal ion was in a *bis*-(2-pyridyl-1,2,3-triazole) environment while the other was in a *bis*-(*bis*-1,2,3-triazole) environment. A 2:2 combination of our other *bis*-bidentate ligand ($\mathbf{L_{pytrz}}$) and Pd(II) also resulted in the formation of a 2+2 macrocycle as a single isomer, which was also cystallographically characterised as the *syn* isomer (Supporting Information S4.5). Pleasingly, the addition of 2 equivalents of $\mathbf{L_{trztrz}}$ to the $[Pd_2(\mathbf{L_{trztrz}})_2]^{4+}$ macrocycle regenerated the $[Pd(\mathbf{L_{trztrz}})_2]^{2+}$ mononuclear complex (Figure 4d).

We had therefore developed a system in which the stoichiometry between ligands and metal ion could be used to switch between a macrocycle and a species with an occluded cationic panel. We now explored whether this could be suited to up or down-regulate the capacity to interact with a molecular target. We carried out NMR titrations between $\mathbf{G_{9MA}}$ and both the mononuclear $[Pd(\mathbf{L_{trztrz}})_2]^{2+}$ and dinuclear $[Pd_2(\mathbf{L_{trztrz}})_2]^{4+}$ species. We found that the macrocycle had higher affinity for the guest than the self-recognising complex, with respective K_{11} values of $220 \pm 10\ M^{-1}$ and $130 \pm 3\ M^{-1}$. We were able to successfully co-crystallise $[Pd_2(\mathbf{L_{trztrz}})_2]^{4+}$ and $\mathbf{G_{9MA}}$, revealing an alternating series of host and guest molecules (Figure 5b). The host displayed the same connectivity as observed in the prior structure, and $\mathbf{G_{9MA}}$ was within range of the planar panel for aromatic π-π interactions (e.g. from the centroid of the central ring and the Pd(II) ion, 3.389 Å). This 1:1 arrangement in the solid state, with hosts with two faces capable of binding two guests, has been observed by us in the past, and is a result of the arrangement giving alternating electron rich-electron poor pairings.[24b,25c]

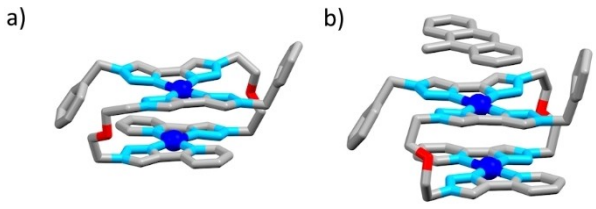

Figure 5. Depictions of X-ray crystal structures of a) $[Pd_2(\mathbf{L_{trztrz}})_2]^{2+}$, and b) $[\mathbf{G_{9MA}} \subset Pd_2(\mathbf{L_{trztrz}})_2]^{4+}$ Colours: carbon grey, nitrogen blue, oxygen red, palladium dark blue. Hydrogen atoms and counterions omitted for clarity.

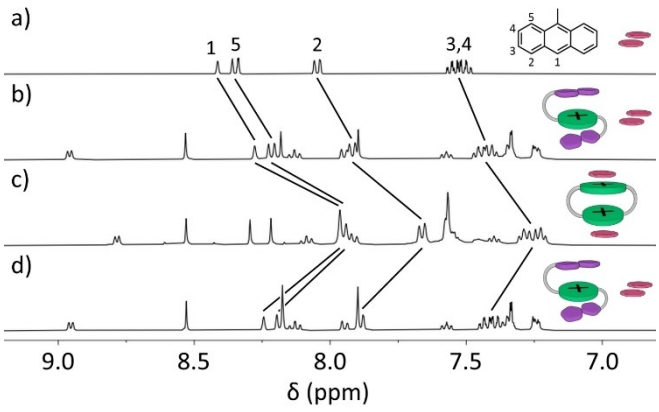

Figure 6. Partial ^{1}H NMR spectra (400 MHz, CD_3CN, 298 K) of a) $\mathbf{G_{9MA}}$, b) $[Pd(\mathbf{L_{trztrz}})_2]^{2+}$ + 2 equivalents $\mathbf{G_{9MA}}$, c) the previous solution + 1 equivalent of Pd(II), giving $[Pd_2(\mathbf{L_{trztrz}})_2]^{4+}$ + 2 equivalents $\mathbf{G_{9MA}}$, and d) the previous solution + 2 equivalents of $\mathbf{L_{trztrz}}$, giving $[Pd(\mathbf{L_{trztrz}})_2]^{2+}$ + 1 equivalents $\mathbf{G_{9MA}}$. Cartoons are designed to show that the affinity for $\mathbf{G_{9MA}}$ has been upregulated or downregulated, rather than turned completely 'on' or 'off'.

With differentiated binding established, we accordingly combined 2 equivalents of $\mathbf{G_{9MA}}$ with self-recognising $[Pd(\mathbf{L_{trztrz}})_2]^{2+}$. The peaks corresponding to the resonances associated with proton environments of $\mathbf{G_{9MA}}$ shifted only slightly upfield, by an average of 0.12 ppm, in the presence of the self-recognising species, $[Pd(\mathbf{L_{trztrz}})_2]^{2+}$ (Figure 6a and b). The addition of a second equivalent of Pd^{2+} produced the macrocyclic species, $[Pd_2(\mathbf{L_{trztrz}})_2]^{4+}$. With 'open' cationic panels and a new-found tetra-cationic charge, the affinity for $\mathbf{G_{9MA}}$ increased, as depicted by significant upfield shifting of the peaks of $\mathbf{G_{9MA}}$ by an average of 0.37 ppm (Figure 6c). The enhanced guest recognition was reversible as the addition of an additional 2 equivalents of ligand to reproduce the species $[Pd(\mathbf{L_{trztrz}})_2]^{2+}$ returned the chemical shifts of the proton environments of $\mathbf{G_{9MA}}$ to close to their original positions (Figure 6d).

Conclusions

The capacity for planar cationic complexes (such as *bis*-(2-pyridyl-1,2,3-triazole)palladium(II) complexes to interact with electron rich aromatic guests through π-π interactions is well established. We have demonstrated that this ability can be impaired through tethering aromatic groups to the complex, where they are able to effectively compete with target guests.

Using a low symmetry *bis*-bidentate ligand with a pyridyl-triazole site at one end and a *bis*-triazole site at the other, we were able to make a mononuclear complex with the tethered and uncomplexed *bis*-triazole sites acting as the self-recognising aromatic groups and occluding access to the cationic panel. Adding more palladium(II) resulted in the formation of a 2+2 macrocycle, and this process was reversible through adding

more ligand. Affinity for 9-methylanthracene could be regulated through switching between the (occluded) mononuclear and (open) dinuclear species. This behaviour is similar in some respects to that observed in biology, where stimuli are able to bring about conformation shifts in flexible systems and open up sites for molecular recognition. We hope to now apply the same approach to larger, more complicated systems, for similar results.

Supporting Information

The authors have cited additional references within the Supporting Information.[29]

Acknowledgements

DP would like to thank the Australian Research Council for a DECRA Fellowship (DE200100421). JA, JP and DP would like to thank the Research School of Chemistry at the Australian National University for additional funding. JP thanks the ANU for an ANU summer research scholarship program. JDE is the recipient of an Australian Research Council Discovery Early Career Award (project number DE220100163) funded by the Australian Government. Phoenix HPC service at the University of Adelaide are thanked for providing high-performance computing resources. This project was undertaken with the assistance of resources and services from the National Computational Infrastructure (NCI), which is supported by the Australian Government. This research was undertaken in part using the MX2 beamline at the Australian Synchrotron, part of ANSTO, and made use of the Australian Cancer Research Foundation (ACRF) detector. Open Access publishing facilitated by Australian National University, as part of the Wiley - Australian National University agreement via the Council of Australian University Librarians.

Conflict of Interests

The authors declare no conflict of interest.

Data Availability Statement

The data that support the findings of this study are available in the supplementary material of this article.

Keywords: self-assembly · metallo-supramolecular · palladium(II) · host-guest chemistry · structural transformation

[1] a) R. A. Laskowski, F. Gerick, J. M. Thornton, *FEBS Lett.* **2009**, *583*, 1692–1698; b) M. F. Perutz, *Q. Rev. Biophys.* **1989**, *22*, 139–237.
[2] For reviews, see; a) K. Harris, D. Fujita, M. Fujita, *Chem. Commun.* **2013**, *49*, 6703–6712; b) T. R. Cook, P. J. Stang, *Chem. Rev.* **2015**, *115*, 7001–7045; c) S. Pullen, J. Tessarolo, G. H. Clever, *Chem. Sci.* **2021**, *12*, 7269–7293.
[3] a) V. Marti-Centelles, A. L. Lawrence, P. J. Lusby, *J. Am. Chem. Soc.* **2018**, *140*, 2862–2868; b) J. Guo, Y. W. Xu, K. Li, L. M. Xiao, S. Chen, K. Wu, X. D. Chen, Y. Z. Fan, J. M. Liu, C. Y. Su, *Angew. Chem. Int. Ed. Engl.* **2017**, *56*, 3852–3856; c) T. Murase, S. Horiuchi, M. Fujita, *J. Am. Chem. Soc.* **2010**, *132*, 2866–2867.
[4] a) J. E. M. Lewis, E. L. Gavey, S. A. Cameron, J. D. Crowley, *Chem. Sci.* **2012**, *3*, 778–784; b) B. Therrien, G. Suss-Fink, P. Govindaswamy, A. K. Renfrew, P. J. Dyson, *Angew. Chem. Int. Ed. Engl.* **2008**, *47*, 3773–3776; c) B.-N. T. Nguyen, J. D. Thoburn, A. B. Grommet, D. J. Howe, T. K. Ronson, H. P. Ryan, J. L. Bolliger, J. R. Nitschke, *J. Am. Chem. Soc.* **2021**, *143*, 12175–12180.
[5] a) M. Yamashina, Y. Sei, M. Akita, M. Yoshizawa, *Nat. Commun.* **2014**, *5*, 4662; b) P. Mal, B. Breiner, K. Rissanen, J. R. Nitschke, *Science* **2009**, *324*, 1697–1699.
[6] W. Wang, Y. X. Wang, H. B. Yang, *Chem. Soc. Rev.* **2016**, *45*, 2656–2693.
[7] a) D. Preston, A. R. Inglis, A. L. Garden, P. E. Kruger, *Chem. Commun.* **2019**, *55*, 13271–13274; b) J. L. Algar, J. A. Findlay, J. D. Evans, D. Preston, *Angew. Chem. Int. Ed.* **2022**, *e202210476*; c) M. Fujita, O. Sasaki, T. Mitsuhashi, T. Fujita, J. Yazaki, K. Yamaguchi, K. Ogura, *Chem. Commun.* **1996**, 1535–1536; d) D. K. Chand, R. Manivannan, H. S. Sahoo, K. Jeyakumar, *Eur. J. Inorg. Chem.* **2005**, *2005*, 3346–3352; e) S. Tashiro, M. Tominaga, T. Kusukawa, M. Kawano, S. Sakamoto, K. Yamaguchi, M. Fujita, *Angew. Chem. Int. Ed. Engl.* **2003**, *42*, 3267–3270; f) D. K. Chand, K. Biradha, M. Kawano, S. Sakamoto, K. Yamaguchi, M. Fujita, *Chem. Asian J.* **2006**, *1*, 82–90; g) X. Lu, X. Li, K. Guo, T. Z. Xie, C. N. Moorefield, C. Wesdemiotis, G. R. Newkome, *J. Am. Chem. Soc.* **2014**, *136*, 18149–18155; h) J.-H. Fu, Y.-H. Lee, Y.-J. He, Y.-T. Chan, *Angew. Chem. Int. Ed.* **2015**, *54*, 6231–6235; i) X. Lu, X. Li, K. Guo, J. Wang, M. Huang, J.-L. Wang, T.-Z. Xie, C. N. Moorefield, S. Z. D. Cheng, C. Wesdemiotis, G. R. Newkome, *Chem. Eur. J.* **2014**, *20*, 13094–13098.
[8] a) M. Fujita, F. Ibukuro, H. Hagihara, K. Ogura, *Nature* **1994**, *367*, 720–723; b) K. Suzuki, M. Kawano, M. Fujita, *Angew. Chem. Int. Ed.* **2007**, *46*, 2819–2822; c) O. Gidron, M. Jirásek, N. Trapp, M.-O. Ebert, X. Zhang, F. Diederich, *J. Am. Chem. Soc.* **2015**, *137*, 12502–12505; d) P. N. Baxter, R. G. Khoury, J. M. Lehn, G. Baum, D. Fenske, *Chem. Eur. J.* **2000**, *6*, 4140–4148; e) J. Ramírez, A.-M. Stadler, N. Kyritsakas, J.-M. Lehn, *Chem. Commun.* **2007**, 237–239; f) B. Kilbas, S. Mirtschin, R. Scopelliti, K. Severin, *Chem. Sci.* **2012**, *3*, 701–704.
[9] a) V. Croue, S. Goeb, G. Szaloki, M. Allain, M. Salle, *Angew. Chem. Int. Ed. Engl.* **2016**, *55*, 1746–1750; b) C. Colomban, G. Szaloki, M. Allain, L. Gomez, S. Goeb, M. Salle, M. Costas, X. Ribas, *Chem. Eur. J.* **2017**, *23*, 3016–3022.
[10] A. K. Chan, W. H. Lam, Y. Tanaka, K. M. Wong, V. W. Yam, *Proc. Natl. Acad. Sci. USA* **2015**, *112*, 690–695.
[11] a) D. Preston, A. Fox-Charles, W. K. Lo, J. D. Crowley, *Chem. Commun.* **2015**, *51*, 9042–9045; b) O. Jurček, P. Bonakdarzadeh, E. Kalenius, J. M. Linnanto, M. Groessl, R. Knochenmuss, J. A. Ihalainen, K. Rissanen, *Angew. Chem. Int. Ed.* **2015**, *54*, 15462–15467; c) R. Zhu, J. Lubben, B. Dittrich, G. H. Clever, *Angew. Chem. Int. Ed. Engl.* **2015**, *54*, 2796–2800.
[12] a) R. Sekiya, M. Fukuda, R. Kuroda, *J. Am. Chem. Soc.* **2012**, *134*, 10987–10997; b) S. Freye, R. Michel, D. Stalke, M. Pawliczek, H. Frauendorf, G. H. Clever, *J. Am. Chem. Soc.* **2013**, *135*, 8476–8479.
[13] a) M. Han, R. Michel, B. He, Y. S. Chen, D. Stalke, M. John, G. H. Clever, *Angew. Chem. Int. Ed. Engl.* **2013**, *52*, 1319–1323; b) R. G. DiNardi, A. O. Douglas, R. Tian, J. R. Price, M. Tajik, W. A. Donald, J. E. Beves, *Angew. Chem. Int. Ed.* **2022**, e202205701; c) A. D. W. Kennedy, R. G. DiNardi, L. L. Fillbrook, W. A. Donald, J. E. Beves, *Chem. Eur. J.* **2022**, *28*, e202104461; d) A. Ghosh, L. Slappendel, B.-N. T. Nguyen, L. K. S. von Krbek, T. K. Ronson, A. M. Castilla, J. R. Nitschke, *J. Am. Chem. Soc.* **2023**, *145*, 3828–3832; e) D. Hugenbusch, M. Lehr, J.-S. von Glasenapp, A. J. McConnell, R. Herges, *Angew. Chem. Int. Ed.* **2022**, *6*, 673–675.
[14] N. Kishi, M. Akita, M. Yoshizawa, *Angew. Chem. Int. Ed. Engl.* **2014**, *53*, 3604–3607.
[15] S. Bandi, S. Samantray, R. D. Chakravarthy, A. K. Pal, G. S. Hanan, D. K. Chand, *Eur. J. Inorg. Chem.* **2016**, *2016*, 2816–2827.
[16] C. F. Espinosa, T. K. Ronson, J. R. Nitschke, *J. Am. Chem. Soc.* **2023**, *145*, 9965–9969.
[17] D. Preston, A. R. Inglis, J. D. Crowley, P. E. Kruger, *Chem. Asian J.* **2019**, *14*, 3404–3408.
[18] D. Preston, P. E. Kruger, *Chem. Eur. J.* **2019**, *25*, 1781–1786.
[19] M. H.-Y. Chan, S. Y.-L. Leung, V. W.-W. Yam, *J. Am. Chem. Soc.* **2019**, *141*, 12312–12321.

[20] a) M. Barboiu, J. M. Lehn, *Proc. Natl. Acad. Sci. USA* **2002**, *99*, 5201–5206; b) A.-M. Stadler, J.-M. P. Lehn, *J. Am. Chem. Soc.* **2014**, *136*, 3400–3409.
[21] a) J. D. Crowley, I. M. Steele, B. Bosnich, *Chem. Eur. J.* **2006**, *12*, 8935–8951; b) S. Ø. Scottwell, A. B. S. Elliott, K. J. Shaffer, A. Nafady, C. J. McAdam, K. C. Gordon, J. D. Crowley, *Chem. Commun.* **2015**, *51*, 8161–8164.
[22] J. L. Algar, J. A. Findlay, D. Preston, *ACS Org. Inorg. AU* **2022**, *2*, 464–476.
[23] D. Preston, *Angew. Chem. Int. Ed.* **2021**, *60*, 20027–20035.
[24] a) F. K. Kong, A. K. Chan, M. Ng, K. H. Low, V. W. Yam, *Angew. Chem. Int. Ed. Engl.* **2017**, *56*, 15103–15107; b) D. Preston, J. A. Findlay, J. D. Crowley, *Chem. Asian J.* **2019**, *14*, 1136–1142; c) R. D. Sommer, A. L. Rheingold, A. J. Goshe, B. Bosnich, *J. Am. Chem. Soc.* **2001**, *123*, 3940–3952; d) J. D. Crowley, A. J. Goshe, B. Bosnich, *Chem. Commun.* **2003**, 2824–2825.
[25] a) D. Preston, P. E. Kruger, *ChemPlusChem* **2020**, *85*, 454–465; b) J. L. Algar, D. Preston, *Chem. Commun.* **2022**, *58*, 11637–11648; c) J. S. Buchanan, D. Preston, *Chem. Asian J.* **2022**, *17*, e202200272.
[26] a) K. A. Stevenson, C. F. C. Melan, O. Fleischel, R. Y. Wang, A. Petitjean, *Cryst. Growth Des.* **2012**, *12*, 5169–5173; b) C. E. Miron, M. R. Colden Leung, E. I. Kennedy, O. Fleischel, M. A. Khorasani, N. Wu, J. L. Mergny, A. Petitjean, *Chem. Eur. J.* **2018**, *24*, 18718–18734; c) K. J. Kilpin, E. L. Gavey, C. J. McAdam, C. B. Anderson, S. J. Lind, C. C. Keep, K. C. Gordon, J. D. Crowley, *Inorg. Chem.* **2011**, *50*, 6334–6346.
[27] Deposition numbers 2279058 (for $[Pd(L_{peg})_2]^{2+}$), 2279057 (for $[Pd(L_{nap})_2]^{2+}$), 2279060 (for $[Pd_2(L_{trztrz})_2]^{4+}$), 2279061 (for $[G_{9MA}\subset Pd_2(L_{trztrz})_2]^{4+}$) and 2279059 (for $[Pd_2(L_{pytrz})_2]^{4+}$) contain the supplementary crystallographic data for this paper. These data are provided free of charge by the joint Cambridge Crystallographic Data Centre and Fachinformationszentrum Karlsruhe Access Structures service.
[28] www.supramolecular.org, this is reported as a 1:2 adduct solely for comparison to other adducts in this study: negligible amounts of the HGG adduct would be present in solution.
[29] a) M. Ouchi, Y. Inoue, Y. Liu, S. Nagamune, S. Nakamura, K. Wada, T. Hakushi, *Bull. Chem. Soc. Jpn.* **1990**, *63*, 1260–1262; b) F. Moradgholi, H. Vahedi, J. Lari, *Org. Commun.* **2015**, *8*, 52–59; c) A. S. Hay, *J. Org. Chem.* **1962**, *27*, 3320–3321; d) in *CrysAlisPro*, Agilent Technologies, Yarnton, England, **2012**; e) G. M. Sheldrick, *Acta Crystallogr. Sect. A* **2008**, *64*, 112–122; f) O. V. Dolomanov, L. J. Bourhis, R. J. Gildea, J. A. K. Howard, H. Puschmann, *J. Appl. Crystallogr.* **2009**, *42*, 339–341; g) D. Aragao, J. Aishima, H. Cherukuvada, R. Clarken, M. Clift, N. P. Cowieson, D. J. Ericsson, C. L. Gee, S. Macedo, N. Mudie, S. Panjikar, J. R. Price, A. Riboldi-Tunnicliffe, R. Rostan, R. Williamson, T. T. Caradoc-Davies, *J. Synchrotron Radiat.* **2018**, *25*, 885–891; h) W. Kabsch, *J. Appl. Crystallogr.* **1993**, *26*, 795–800; i) in *Spartan '16*, Wavefunction, Inc., Irvine, CA, **2016**; j) F. Neese, *Wiley Interdiscip. Rev.: Comput. Mol. Sci.* **2022**, e1606; k) J. P. Perdew, W. Yue, *Phys. Rev. B* **1986**, *33*, 8800–8802; l) F. Weigend, R. Ahlrichs, *Phys. Chem. Chem. Phys.* **2005**, *7*, 3297–3305; m) P. Pollak, F. Weigend, *J. Chem. Theory Comput.* **2017**, *13*, 3696–3705; n) D. Andrae, U. Häußermann, M. Dolg, H. Stoll, H. Preuß, *Theor. Chim. Acta* **1990**, *77*, 123–141; o) S. Grimme, S. Ehrlich, L. Goerigk, *J. Comput. Chem.* **2011**, *32*, 1456–1465; p) A. Jerschow, N. Müller, *J. Magn. Reson. Ser. A* **1996**, *123*, 222–225; q) A. Jerschow, N. Müller, *J. Magn. Reson.* **1997**, *125*, 372–375.

Manuscript received: August 1, 2023
Revised manuscript received: August 28, 2023
Accepted manuscript online: August 29, 2023
Version of record online: September 11, 2023